sustainability

MDPI

Article

Model Test Study on Natural Thawing Temperature Field of Artificial Ground Frozen Wall

Haibing Cai [1,*], Longfei Yang [1], Changqiang Pang [1], Mengkai Li [1], Chanrui Lu [1] and Rongbao Hong [1,2]

[1] School of Civil Engineering and Architecture, Anhui University of Science and Technology, Huainan 232001, China
[2] School of Architectural Engineering, Nantong Vocational University, Nantong 226007, China
* Correspondence: haibingcai@163.com; Tel.: +86-139-6645-0807

Abstract: In order to visualize the evolution and distribution law of the ground temperature field during artificial freezing construction, an indoor model test study was carried out based on the independently constructed hygrothermal coupling artificial ground freezing test platform. The test results show that the soil temperature in the freezing process went through the three stages of a steep drop, a slow drop, and stabilization, the earliest closure position of the frozen wall was the intermediate point between two freezing pipes, and the thickness of the frozen wall on different sections showed Section 1 > Section 2 > Section 3 after 61 min of positive freezing. The soil temperature in the natural thawing process went through the four stages of a rapid rise, short hysteresis, a second rapid rise, and a linear slow rise. By fitting the test data, the distribution function of the pipe wall temperature along the pipe length under natural thawing conditions was obtained. The research results can provide a valid basis for the numerical calculation model of a three-dimensional non-uniform natural thawing temperature field and can also provide a reference for the design of settlement grouting under natural thawing conditions.

Keywords: artificial ground freezing method; hygrothermal coupling; model test; temperature field

check for updates

Citation: Cai, H.; Yang, L.; Pang, C.; Li, M.; Lu, C.; Hong, R. Model Test Study on Natural Thawing Temperature Field of Artificial Ground Frozen Wall. *Sustainability* **2023**, *15*, 3186. https://doi.org/10.3390/su15043186

Academic Editors: Hong Wong, Vasilis Kanakoudis, Dan Ma, Lang Liu, Jiangyu Wu and Wen Zhong

Received: 21 December 2022
Revised: 28 January 2023
Accepted: 29 January 2023
Published: 9 February 2023

1. Introduction

Artificial ground freezing technology is used to form an impermeable permafrost layer by freezing the water in the soil into ice, which plays the role of groundwater isolation and reinforcement to the strata, with the superiority of good sealing, high strength, rigidity, and environmental protection, and has been widely used in recent years [1,2], especially in the construction of tunnels, which are an essential part of metro cities [3]. The thickness of the frozen wall is an indicator to judge whether the freezing effect meets the subsequent construction conditions [4], which is obtained through the distribution of the temperature field of the stratum. When the construction of the lining structure is completed, the frozen wall needs to be thawed naturally or forcibly, and the hot thawing effect caused by the melting of the frozen soil and the soil drainage consolidation caused by water migration will cause the ground to deform and move, and the thawing settlement effect is more obvious than the frost heave effect [5].

In terms of field measurement analysis, Yang et al. [6] provided the relationship between the average temperature, thawing rate, and thawing time based on field monitoring data. Hu et al. [7,8] concluded that the deformation of the stratum could be controlled within a reasonable range by controlling the forced thawing rate in pipe-roofing freezing construction in a timely manner. Ma et al. [9] combined the field monitoring data and numerical simulation results to establish a preliminary relationship between the thawing temperature and the thawing time. Levin et al. [10] found that the natural thawing of frozen rock can be maintained for decades by monitoring the thawing process of the frozen wall of the Petrikov potash mine. In terms of theoretical analysis, Li et al. [11] introduced an exponential integral function to derive the analytical solution related to the extension rate, thinness, and time of a frozen wall. Jiang et al. [12] established the mathematical analytical solution of a single-pipe freezing temperature field by solving the heat conduction equation using variable substitution and expressed the temperature change in the thawing zone as a polynomial function. Zhang et al. [13] established the prediction equation of a forced thawing temperature field related to the thawing front radius, heat flow density, and average thawing temperature. Cai et al. [14,15] derived the single-pipe thawing theory and flat-plate thawing theory based on heat transfer theory and verified that the temperature field variation of forced thawing can be explained by the single-pipe thawing theory. In terms of numerical simulation, Harlan [16] established a physical model of hydrothermal coupling by considering the joint action of moisture and temperature fields for the first time in 1973. Chen et al. [17] established a semi-empirical hydrothermal coupling model by integrating the empirical equations of freezing and swelling. Later, Shen and Branko [18] established a simplified hydrothermal coupling mathematical model of frozen soil and considered the connection of the temperature field, deformation field, and moisture field. Yuan et al. [19] used ADINA software to simulate a freezing construction of a shield tail brush replacement and found that when the brine temperature of forced thawing was maintained at 60~80 °C, the thawing time was shortened with the increase in the brine temperature. Chen et al. [20] found that the forced thawing time was positively correlated with the thermal conductivity and specific heat capacity of soil by simulating the freezing construction of a crossing-river tunnel. Fu et al. [21] explored the longitudinal and radial temperature field distribution of the stratum during the natural thawing process of an artificial freezing tunnel and analyzed the sensitivity of thermal conductivity and latent heat and the ambient temperature to the temperature field distribution. In terms of experimental research, Zhou et al. [22] carried out centrifugal model tests of ground freezing and thawing under 1 g and 30 g conditions and found that the movement rate of the thawing front under the 30 g condition was a power exponential function of the thawing time, not the square root relationship under general conditions. Shi et al. [23] carried out a model test on freezing reinforcement for a shield junction and found that the average development rate of frozen soil inside freezing pipes was approximately 1.5 times that of outside. After completing freezing, the average temperature of the internal frozen soil was approximately 1.9 times that of the outside. Hu et al. [24] conducted a large physical model test of a freeze-sealing pipe roof and found that the method freezes faster and is more resistant to thermal weakening of excavation. Based on the principle of equivalent cooling capacity, Duan et al. [25] designed the FSPR model test of double circular freezing pipes, which shows that the improved design can effectively replace the original design of the profiled freezing pipe by comparing the temperature field distribution.

In summary, most of the existing research focuses on the predictive and influencing factors of frozen wall development and the distribution law of the temperature field. Furthermore, the analysis object is primarily the radial section of the frozen wall, while the study of the temperature field distribution along the length of the freezing pipe has not been reported. To this end, similar model tests were conducted based on the hygrothermal coupling criterion and using an artificial ground freezing test platform built independently to investigate the evolution law of the temperature field of the stratum and its distribution law during the natural thawing process. This research can provide a reference for the subsequent verification of the numerical calculation method and the field control of thawing settlement.

2. Design of Model Test

2.1. Project Overview

An underground interval tunnel in Beijing was constructed under difficult conditions due to the leakage of water pipes in the overlying strata and years of disrepair, serious seepage of water from the strata resulting in a decrease in the strength of the strata, and a complex ground traffic environment. For this reason, the interval section was constructed using local freezing reinforcement and the concealed excavation method. Among them, the tunnel burial depth is 10.0 m, the excavation barren diameter is 3.0 m, and a 2.0 m thick layer of saturated sandy soil with a high permeability coefficient exists at the vault. Eight seamless steel pipes with a diameter of 108 mm, a length of 15.0 m, and a wall thickness of 5mm were used as freezing pipes, with a spacing of 0.68 m between adjacent freezing holes and a distance of 0.3 m from the tunnel excavation boundary. The frozen wall was designed to be 1.2 m thick with an average temperature of −10 °C, the brine temperature during positive freezing was −24~−26 °C, the positive freezing time was 38 d, and the natural thawing time was 53 d.

2.2. Derivation of Similarity Criteria

The model test is a prototype similarity test carried out under an isometric or scaled-down model and meeting the corresponding similarity criteria (temperature field criteria, moisture field criteria, etc.) is a prerequisite for the successful completion of the above-mentioned test. For this reason, this study selects the typical soil environment of the construction section for the local vertical freeze–thaw model test and selects the equation analysis method to determine the similarity criterion as follows.

2.2.1. Similarity Criterion of Temperature Field

The differential control equation for the thermal conductivity of the soil is

$$\frac{\partial t_n}{\partial \tau} = a_n\left(\frac{\partial^2 t_n}{\partial r^2} + \frac{1}{r}\frac{\partial t_n}{\partial r}\right) \quad (0 < r_0 < r < \infty, \tau > 0, n = 1, 2) \tag{1}$$

where r is the radial coordinate; τ is time; t_n is the temperature at point r, the unfrozen zone at n = 1, and the frozen zone at n = 2, and α_n is the thermal diffusion coefficient of the soil.

The initial and boundary conditions for the temperature field are

$$\begin{cases} \tau = 0, t(r) = t_0 \\ \tau > 0, t(r_0) = t_y, t(\rho) = t_d, t(\infty) = t_0 \end{cases} \tag{2}$$

where t_0 is the initial temperature of the soil, r_0 is the radius of the freezing pipe, ρ is the coordinate of the outer surface of the frozen wall, t_d is the freezing temperature of the soil, and t_y is the temperature of the freezing pipe wall.

The heat balance equation at the thawing front (r = ρ) is

$$\lambda_2 \frac{\partial \theta_2}{\partial r}\Big|_{r=\rho} - \lambda_1 \frac{\partial \theta_1}{\partial r}\Big|_{r=\rho} = L\frac{d\rho}{d\tau} \tag{3}$$

where λ is the thermal conductivity of soil and L is the latent heat of phase change of soil.

According to Equations (1)–(3), the similarity criterion for the soil temperature field can be obtained by equation analysis as

$$F(F_T, K_T, R, \theta) = 0 \tag{4}$$

where F_T is the Fourier criterion, $F_T = \frac{a\tau}{r^2}$; K_T is the Kosovich criterion, $K_T = \frac{L}{ct}$; c is the specific heat capacity of soil; t is the temperature; R is the geometric criterion; θ is the temperature criterion, $\theta = T_r/T_0 = T_c/T_0$; and T_r and T_c are the average temperature of the frozen wall and the brine temperature, respectively. To reduce the test error, the soil used in this study is taken from the engineering site, so C_a = C_c = 1, and the mass water content is the same, while the latent heat generated by the ice–water phase change in the soil is equal, substituting it into Equation (4) to obtain

$$C_\tau = C_r^2 \tag{5}$$

$$C_t = 1,\ t = t' \tag{6}$$

From Equation (5), the time similarity ratio in the model test is the square of the geometric similarity ratio, C_r is the geometric similarity ratio, and C_τ is the time similarity ratio; from Equation (6), the temperature in the similarity test and the engineering reality remain the same, so the temperature similarity ratio is 1.

2.2.2. Humidity Field Similarity Criterion

Moisture migration will occur in the stratum during the freezing process due to the presence of a moisture field. Its differential control equation is as follows:

$$\frac{\partial h}{\partial \tau} = b\left(\frac{\partial^2 h}{\partial r^2} + \frac{1}{r}\frac{\partial h}{\partial r}\right) \tag{7}$$

The initial and boundary conditions for the humidity field are

$$\begin{cases} \tau = 0, h = h_0 \\ \tau > 0, h(h = \infty) = h_0, h(h = \rho) = 0 \end{cases} \tag{8}$$

where h is the moisture content and b is the moisture conductivity.

Based on Equations (7) and (8), the equation of similarity criterion for the soil moisture field is determined by equation analysis as

$$F(F_h, R, H) = 0 \tag{9}$$

where H is the moisture criterion and F_h is the moisture field Fourier criterion, $F_h = \frac{b\tau}{r^2}$.

From the above equation, the moisture migration process and the soil freezing process are mathematically modeled similarly and both obey the Fourier criterion. Therefore, under geometrically similar conditions, when the temperature field is consistent, the humidity field is also consistent. Based on the derived similarity criterion, the similarities of the most critical parameters in the model tests are shown in Table 1.

Table 1. Similarity constant of the model test.

Parameters	Geometry	Time	Temperature	Humidity	Unit Weight
Ratio of similitude	30	900	1	1	1

2.3. Model Test System

Considering the boundary conditions of actual engineering, the model test box size, and the layout of freezing pipes, the geometric similarity ratio of this model test is taken to be C_r = 30 and the model test box specification is shown in Figure 1.

The test relies on the self-built platform for the artificial-ground freezing–thawing test in tunnels, including the model test box, freezing system, and data acquisition system, as shown in Figure 2.

(1) Model test box

As shown in Figure 3a, the model test box is 1000 mm × 600 mm × 900 mm (length × width × height), the box is made of a Q235 steel plate welded with a thickness of 10 mm, and the welded area is treated with waterproofing so that the box has good resistance to pressure and water. To avoid boundary effects, that is, gaps arising between the soil and the box boundary during the test, which would lead to water flowing in the direction of less resistance (box boundary) and ultimately produce large test errors, a layer of anti-rust paint was evenly applied to the inside and outside of the model test box, and a layer of black plastic waterproofing and an insulation membrane was laid on the bottom and sides.

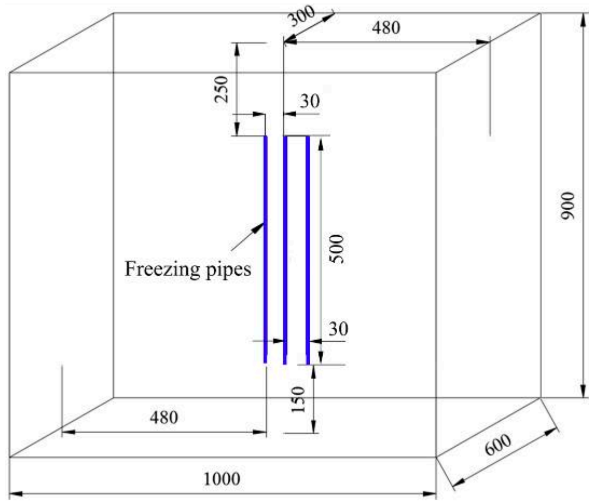

Figure 1. Layout of freezing pipes (Unit: mm).

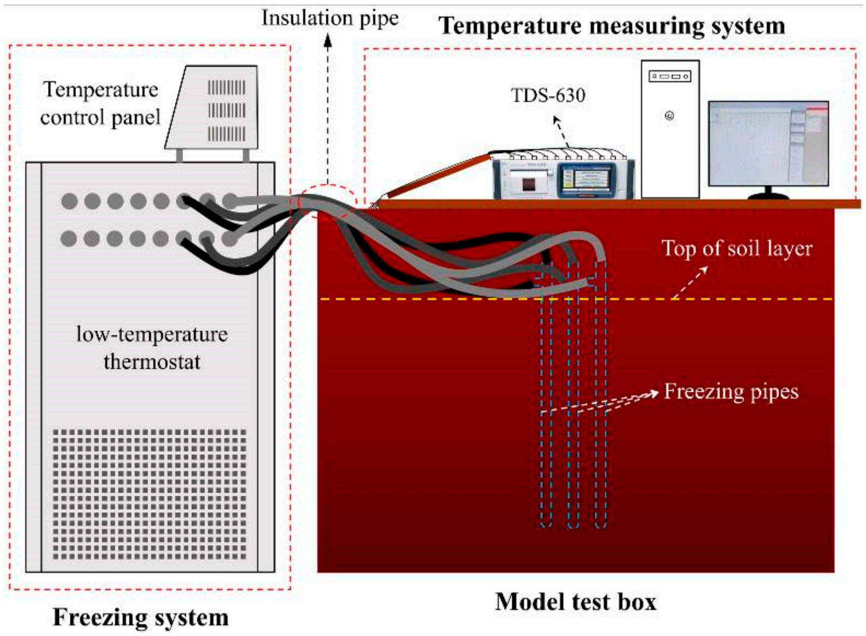

Figure 2. Model test system.

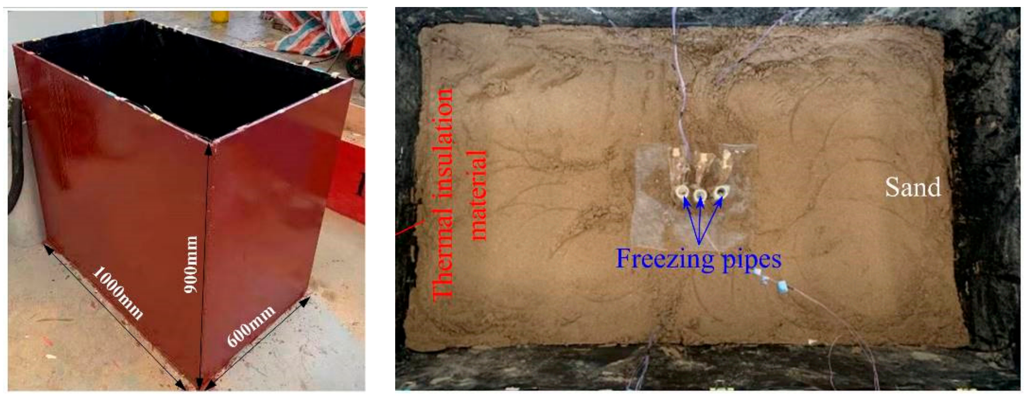

(**a**) (**b**)

Figure 3. Model test box: (**a**) External surface of box; (**b**) internal condition of box.

As shown in Figure 3b, the model test box was filled with saturated fine sand to a height of 650 mm, and the basic physical and thermophysical parameters of the fine sand are shown in Tables 2 and 3.

Table 2. Basic physical parameters of soil.

Parameters	Water Content (%)	Density (kg·m^{-3})	Specific Gravity	Porosity (%)	Particle Size (mm)
Sand	18.25	1950	2.70	0.74	0.3~0.5

Table 3. Thermophysical and mechanical parameters of soil.

Parameters		Thermal Conductivity (kcal·m^{-1}·d^{-1}·°C^{-1})	Specific Heat (kcal·kg^{-1}·°C^{-1})	Latent Heat of Phase Change (kcal·kg^{-1})	Freezing Temperature (°C)	Elastic Modulus (MPa)	Poisson Ratio
Sand	Unfrozen	23.00	0.357	8.93	−0.5	15	0.29
	Frozen	38.06	0.240			45	0.23

(2) Freezing system

As shown in Figure 4a, the NDC-4015Z low-temperature thermostat produced by Hengnuo Instrument Manufacturing Co., Ltd. from Suzhou, Jiangsu Province, China was used. The device can achieve a temperature control cycle of −120~300 °C and the temperature error is only ±0.1 °C. To avoid corrosion of the device by brine and to prolong its service life, ethylene glycol with a purity of 97% (a freezing temperature of −110 °C and a boiling temperature of 78 °C) was used as the circulating refrigerant. Three sleeve-type freezing pipes (Figure 4c) with an external diameter of 10 mm and a length of 500 mm were used for the test, and they were placed vertically at 30 mm intervals along the length direction of the box, with a distance between the end of the freezing pipes and the bottom of the box of 150 mm.

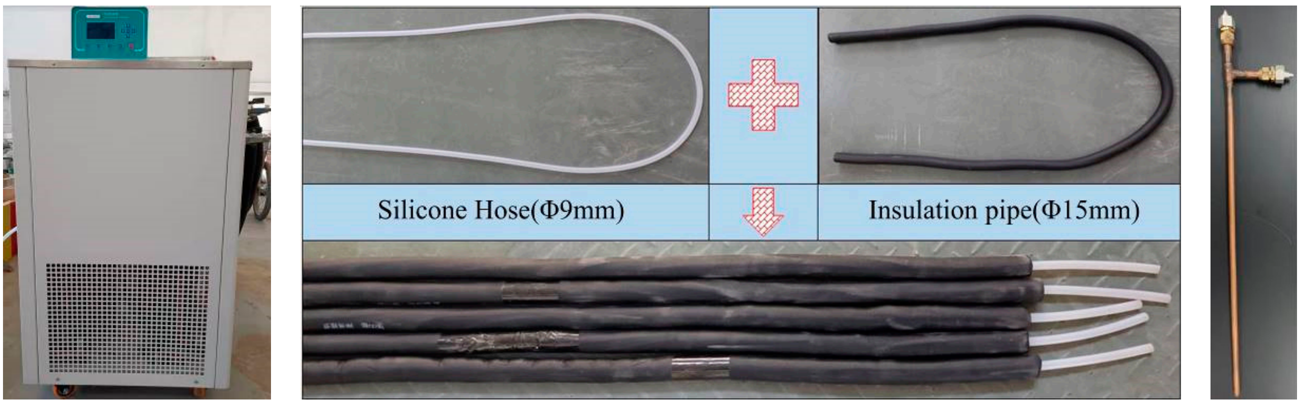

(**a**) (**b**) (**c**)

Figure 4. Freezing system: (**a**) Low-temperature thermostat; (**b**) insulation pipe; (**c**) freezing pipe.

(3) Temperature measuring system

As shown in Figure 5, three horizontal planes of 50, 250, and 450 mm (from the bottom to the top) from the end of the freezing pipe were selected as temperature-measuring sections, with eight soil measuring points that were located at the edge of the designed frozen wall and one pipe wall measuring point on each section. The temperature measuring elements were selected from a Kang Cu-Cu thermocouple string, and the temperature data were collected using a TDS-630 multi-point data acquisition instrument with a frequency of 1 min.

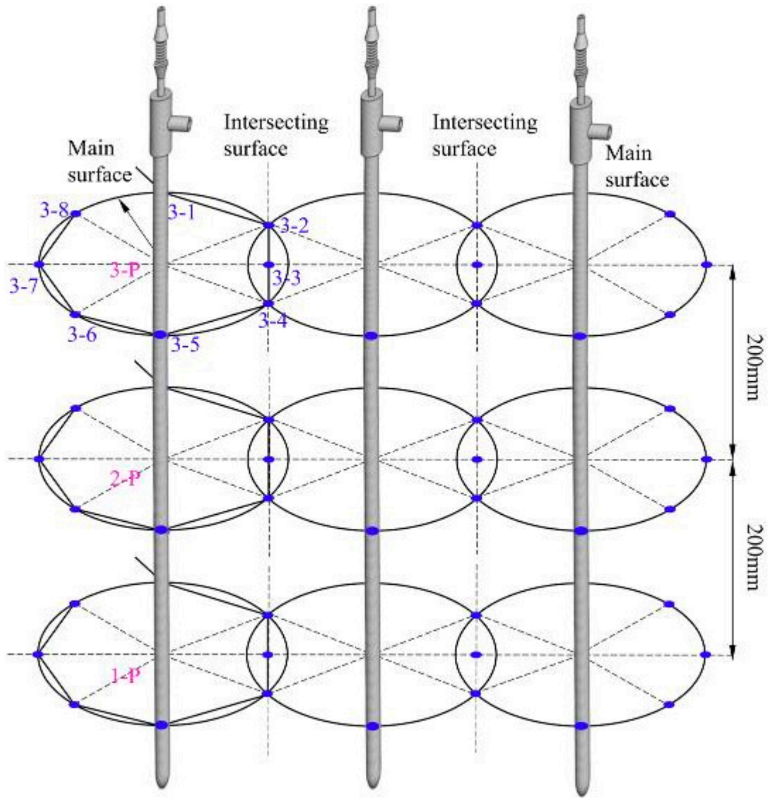

Figure 5. Layout of temperature-measuring points.

2.4. Temperature Setting

The positive freezing time was 61 min, during which the alcohol temperature was set to –24 °C, then the freezing was maintained at a temperature of −21 °C for 7 min, and finally, the circulation of alcohol was stopped to allow the stratum to thaw naturally for 85 min.

3. Analysis of Test Results

3.1. Evolution Law of Freezing Temperature

The temperature history curves of each measuring point in different sections are shown in Figure 6. Figure 6a–c show that the temperature changes of all measuring points in the three sections during the freezing process went through three stages: A steep drop, a slow drop, and basic stability. At the beginning of freezing, the temperature of each measuring point in the soil decreases rapidly, and as freezing continues, phase changes occur in the soil near the freezing pipes, latent heat is released, the freezing front extends outward with the freezing pipes at the center, and the cooling rate gradually decreases and eventually stabilizes.

After positive freezing for 61 min (corresponding to approximately 38 days), the temperature of all measuring points reaches below the freezing temperature, indicating that the thickness of the frozen wall reached the design requirements. After freezing for 72 min (corresponding to 45 days), the temperature of each measuring point was essentially stable. Due to the thermal potential superposition effect at the interface position, the cooling effect of measuring points 1-2, 1-3, and 1-4 is obviously better than that of other measuring points in the soil, and their final temperatures are also lower. Secondly, the temperature drop curves of symmetrical measuring points (such as 1-1 and 1-5, 1-2 and 1-4, and 1-6 and 1-8) essentially coincide, and the average cooling rates at the three sections can reach 0.467, 0.451, and 0.438 °C/min, respectively. It shows that the freezing pipes and thermocouple string positioning are more accurate, and the test results are credible.

As shown in Figure 6d, the cooling curves of the freezing pipe walls at different sections are essentially the same, which all experience two stages of initial steepness and subsequent gentleness. Due to the arrangement and size of the freezing pipe, the temperature of the pipe wall in the steady state is slightly different, which is −13.4 °C (Section 1), −12.6 °C (Section 2), and −11.2 °C (Section 3), respectively.

To understand the development of the frozen wall, the cloud map of the freezing temperature field at different sections after positive freezing for 61 min is drawn as shown in Figure 7.

After freezing for 61 min, the frozen wall completely closes, and the thickness of the frozen wall at three sections is 77.19, 76.31, and 63.13 mm, respectively. The average thickness is more than 40 mm (corresponding to 1.2 m), which meets the engineering design requirements. The frozen wall temperatures range from –13.4~–2.1 °C at Section 1, −12.6~−1.3 °C at Section 2, and −11.2~−0.5 °C at Section 3. The thickness of the frozen wall in three sections is shown as Section 1 > Section 2 > Section 3, that is, the closer to the end of the freezing pipe, the better the freezing effect of the soil is. In addition, the temperature gradient of the soil between freezing pipes is greater than that outside the freezing pipes due to the superposition of thermal potentials, and the temperature gradient of the soil in the direction of the axis of freezing pipes is greater than that in the direction of the vertical axis.

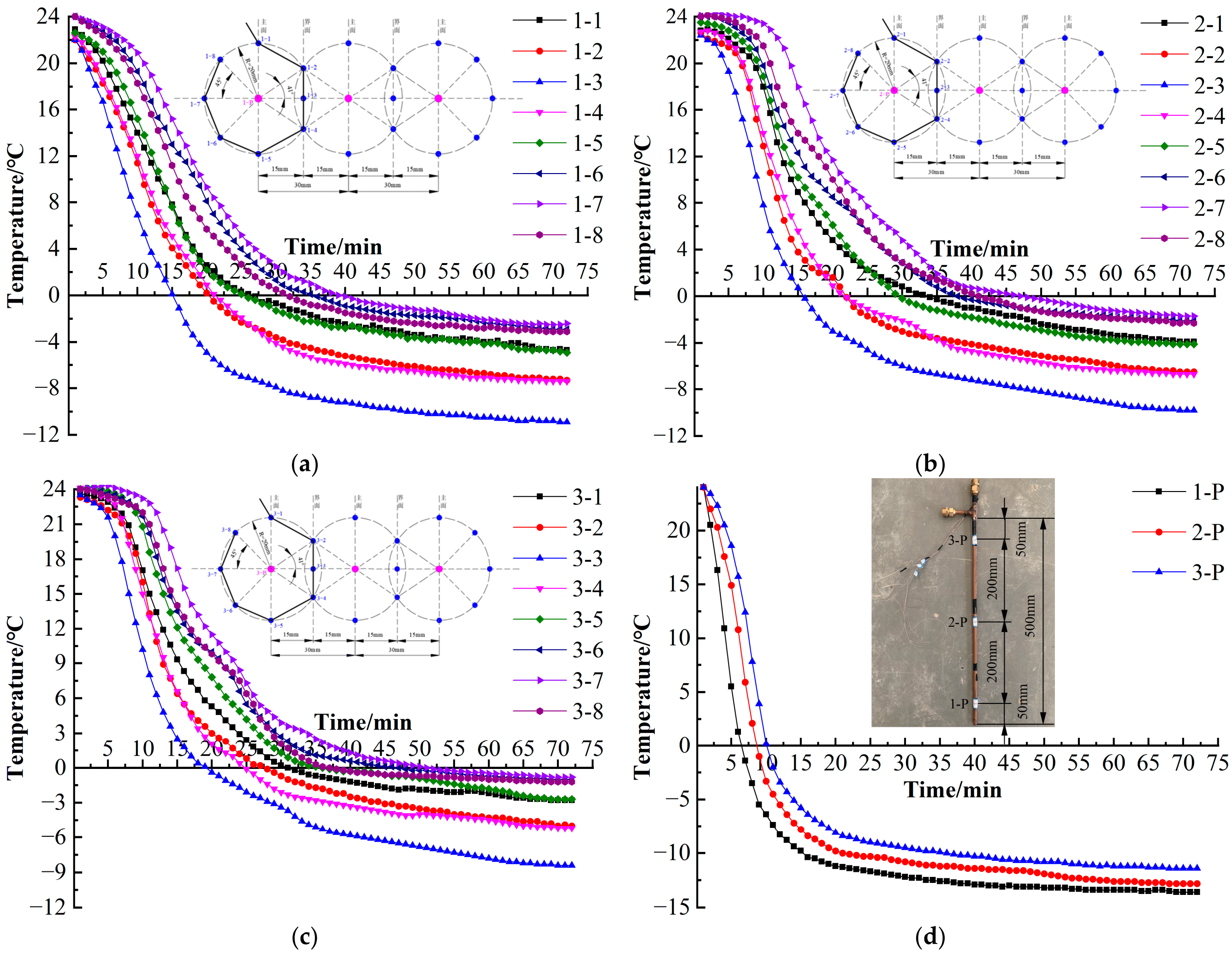

Figure 6. Temperature duration curve of measuring points on each section during freezing: (**a**) Section 1; (**b**) Section 2; (**c**) Section 3; (**d**) freezing pipe wall.

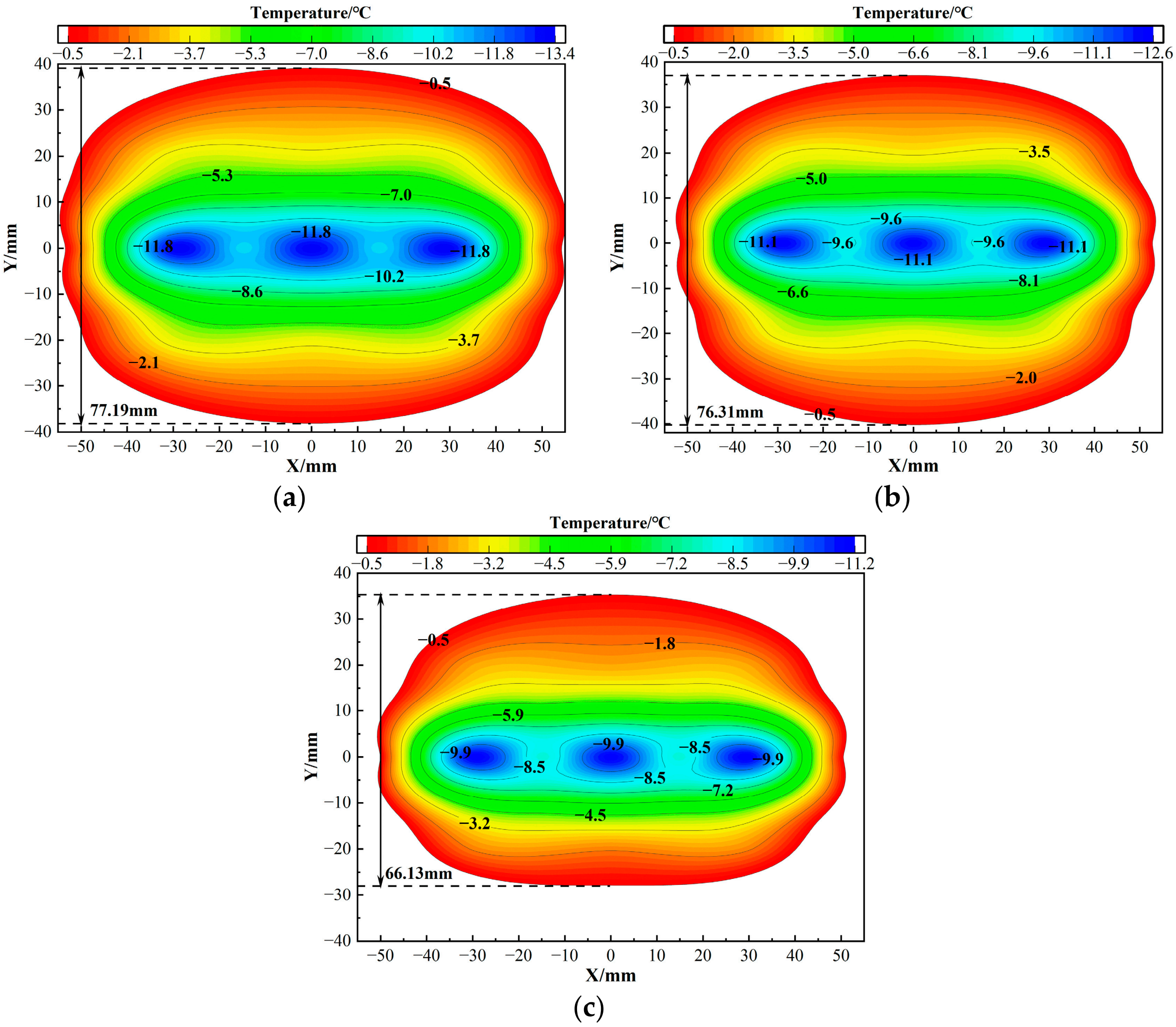

Figure 7. Temperature field distribution at each section after positive freezing for 61 min: (**a**) Section 1; (**b**) Section 2; (**c**) Section 3.

3.2. Evolution Law of Thawing Temperature

3.2.1. Temperature History Change

The temperature change law of the measuring points at each section during natural thawing is shown in Figure 8. When the maintenance freezing ends and the cooling is stopped, the soil begins to thaw naturally, and as time advances, the temperature change in all three sections goes through four stages: A rapid rise, a transitory lag, a second rapid rise, and a linear slow rise. As shown in Figure 8a–c, at the beginning of natural thawing, the temperature of all measuring points rises rapidly. When it is about to rise to 0 °C, the frozen soil absorbs a large amount of heat due to the phase change, the rate of temperature rise slows down, and then a transitory lag in temperature change occurs. Next, the temperature continues to rise rapidly again, and when the temperature reaches 11 °C, the rate of temperature rise enters a stable phase until it returns to an ambient temperature. After natural thawing for 85 min (corresponding to 53 days), the frozen wall disappears completely and the soil essentially returns to its initial temperature, and the time of thawing is approximately 1.39 times longer than that of positive freezing (61 min).

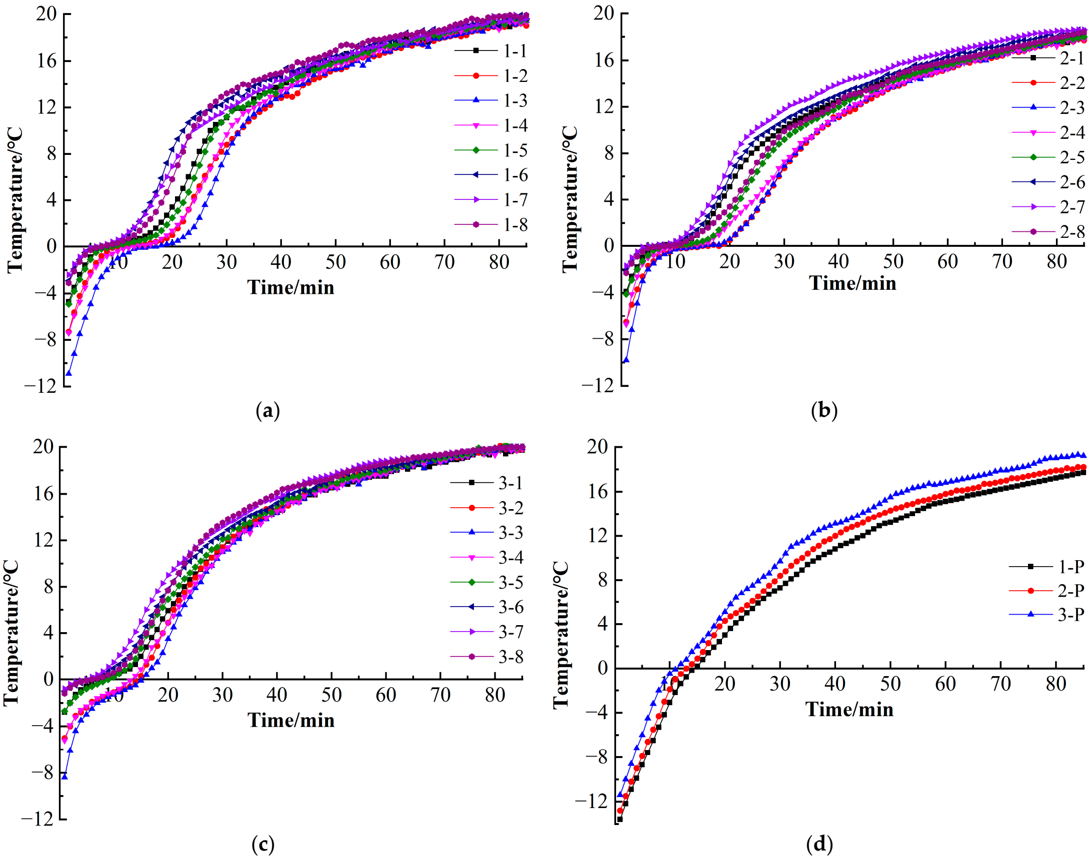

Figure 8. Temperature change curve of measuring points at each section during natural thawing: (**a**) Section 1; (**b**) Section 2; (**c**) Section 3; (**d**) freezing pipe wall.

At the beginning of thawing, the starting temperatures of measuring points 1-3, 2-3, and 3-3, which are located at the intersection surface of the frozen wall, are the lowest, but under the influence of a large temperature gradient, their warming is significantly faster than that of other measuring points in the soil, and the temperatures at the later stages of thawing were also very close to those of other measuring points. The point with the fastest temperature rise is similar to the freezing process, which is still the connection midpoint of freezing pipes, and the average warming rates of the measuring point at three sections were 0.361, 0.348, and 0.334 °C/min, respectively. Secondly, as Section 3 is close to the top of the soil layer, the heat exchange with the atmosphere is more intense. Furthermore, the phase transition interval of the temperature change at each measuring point is shorter and the lag time is significantly shorter than that at Section 1 and Section 2. However, it can still be seen that the curvature of the temperature increase curve changes near the phase-change temperature, and the final temperature of the measuring points in Section 1 is slightly higher than that in Section 2 and Section 3.

As shown in Figure 8d, the temperature change curve of the pipe wall does not show any hysteresis during natural thawing, only a rapid rise stage before the phase change of the soil and a slow rise stage with an approximate power function distribution after the phase change. After completing thawing, the final temperatures at three measuring points 1-P, 2-P, and 3-P are 19.5 °C, 18.5 °C, and 18 °C in that order, showing that the greater the depth of burial, the lower the temperature is.

3.2.2. Evolution Law of Horizontal Thawing Temperature Field

To visualize the natural thawing process of the frozen wall, cloud maps of thawing temperature fields at three sections after thawing for 5, 15, 48, and 85 min (corresponding to the actual 3, 9.4, 30, and 53 days) are drawn, as shown in Figure 9.

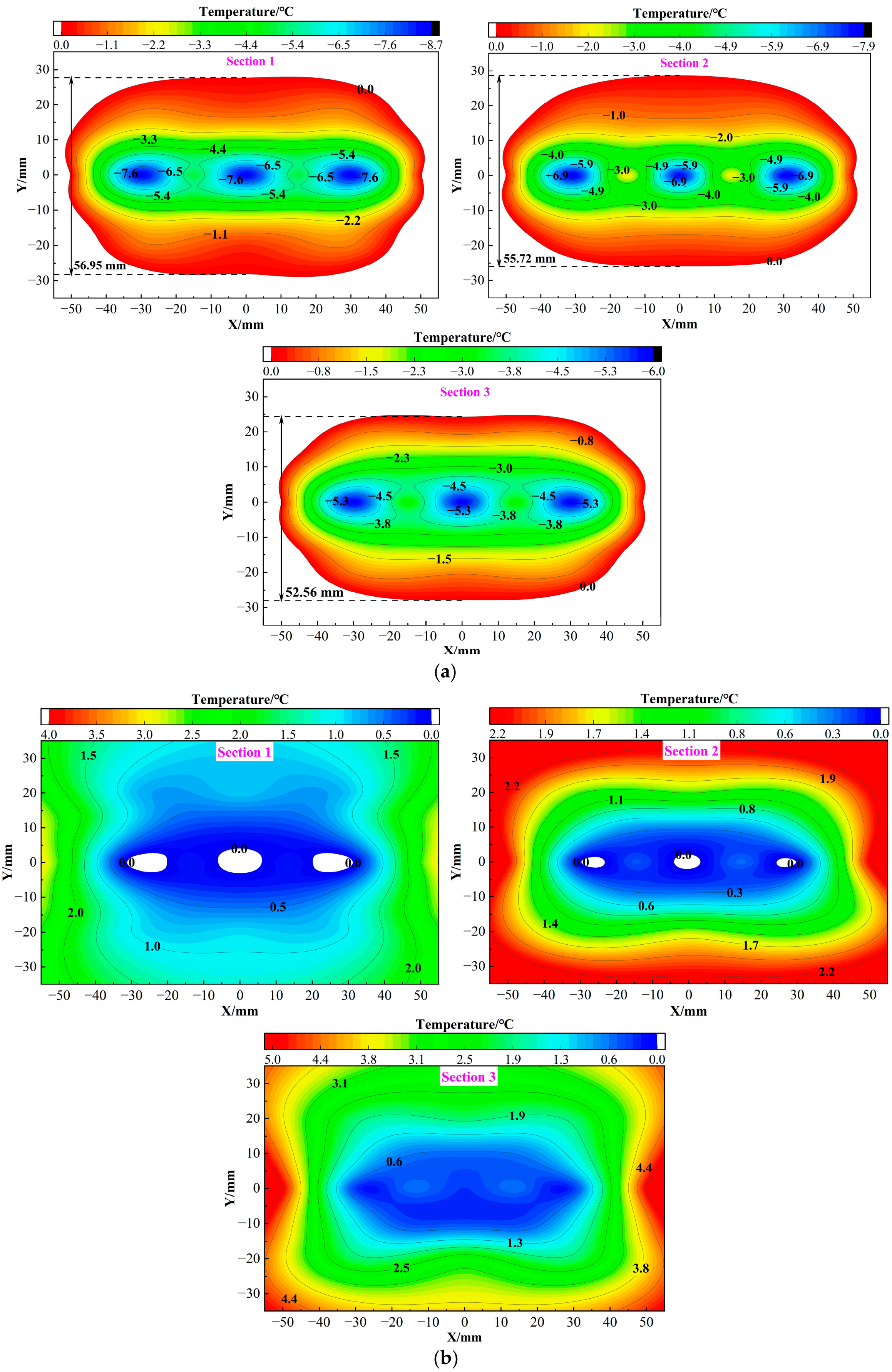

Figure 9. *Cont.*

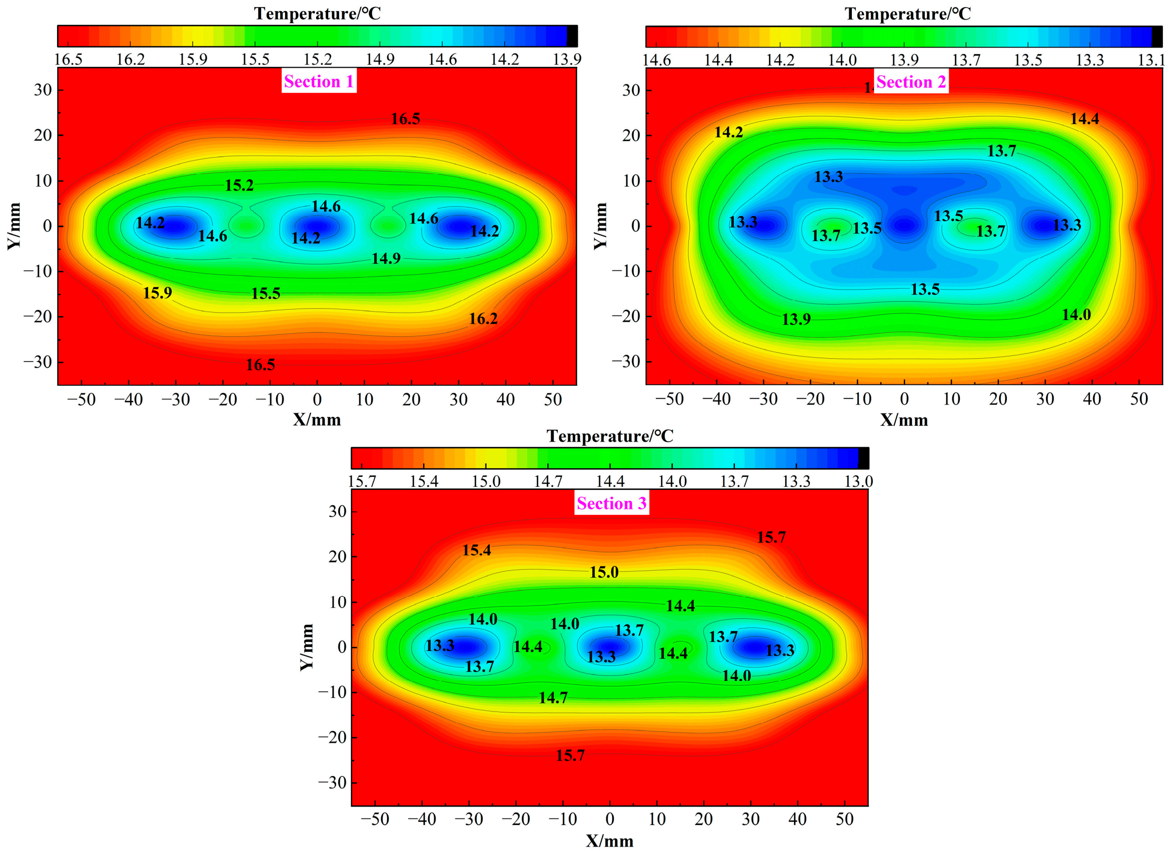

(**c**)

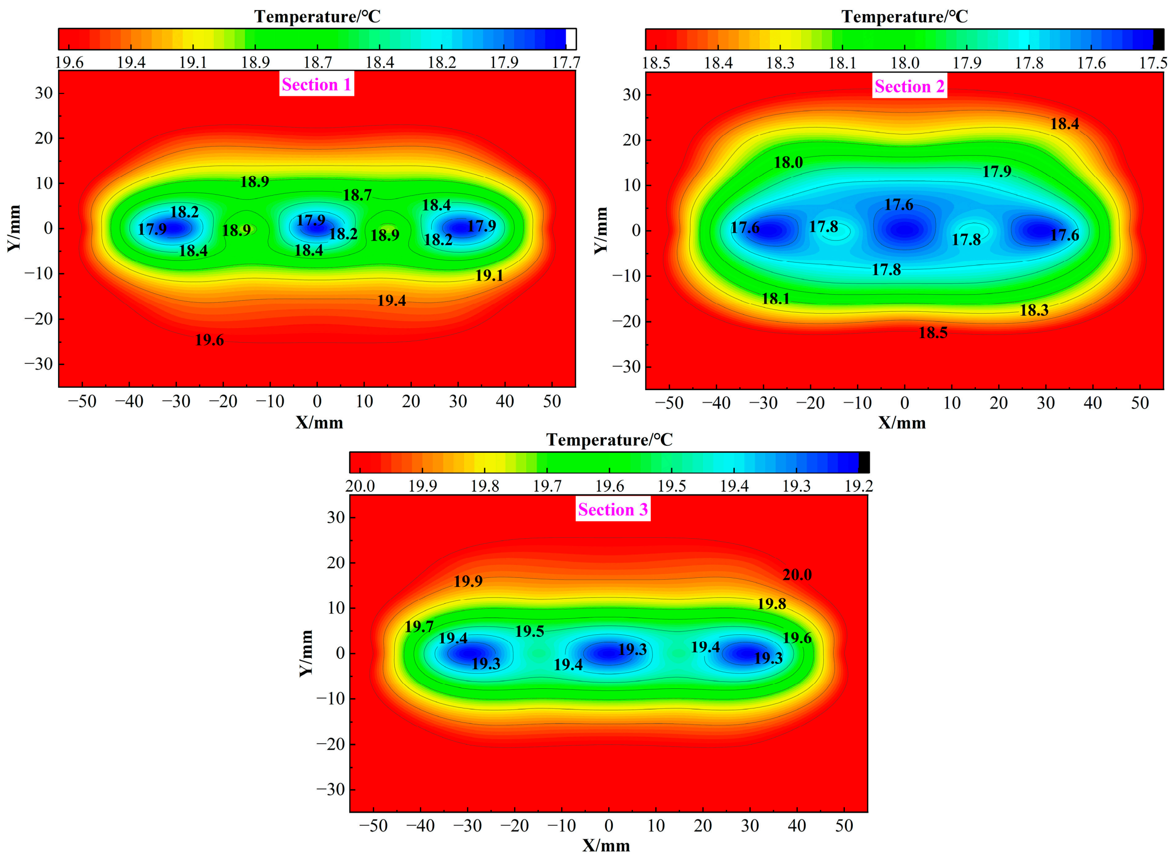

(**d**)

Figure 9. Temperature field distribution at three sections after thawing for different times: (**a**) 5 min; (**b**) 15 min; (**c**) 48 min; (**d**) 85 min.

After thawing for 5 min, the frozen walls at three sections all have an obvious shrinkage, with temperatures starting from –8.7~0 °C and thicknesses decreasing to 56.95, 56.72, and 52.56 mm, respectively. After thawing for 15 min, the frozen walls in three sections thawed considerably. The frozen wall at Section 3 closest to the top of the soil layer has completely disappeared, while there are still fine frozen soil columns (blank area) around freezing pipes at Section 1 and Section 2, and the whole frozen wall completely disappears after thawing for approximately 18 min (11.25 days). After thawing for 48 min, the soil and the pipe wall warmed up further, with temperatures in the thawing zone ranging from 13.0 to 15.7 °C, 13.1 to 14.6 °C, and 13.9 to 16.5 °C at three sections, respectively. After thawing for 85 min, the temperatures of the measuring points at three sections are between 17.5 °C and 20 °C, and the thawing essentially meets the requirements.

At the beginning of thawing, the temperature gradient between adjacent freezing pipes is larger, but the isotherms on the outside of pipes became dense after completing thawing, showing the temperature gradient on the outside of pipes is instead larger than that between pipes, which is the opposite of the result after completing positive freezing. In addition, Section 3 has a more intense heat exchange due to it being closest to the top soil layer, resulting in the average temperature in the thawing area being significantly higher than the other two sections. Section 1, although forming the thickest frozen wall, is close to the unfrozen soil layer below and has the second highest heat exchange efficiency with the surrounding stratum only after Section 3. Section 2 is in the middle part of the soil layer and has the lowest heat exchange efficiency with the surrounding stratum. As a result, after 85 min of natural thawing, the scale of the area below 20 °C (initial ground temperature) in three sections is Section 3 < Section 1 < Section 2.

3.2.3. Evolution Law of Vertical Thawing Temperature Field

By comparing the horizontal thawing temperature field, it can be found that the frozen wall morphology and temperature distribution differ in three sections. Similarly, the vertical temperature fields of the soil layer at different thawing moments are shown in Figure 10.

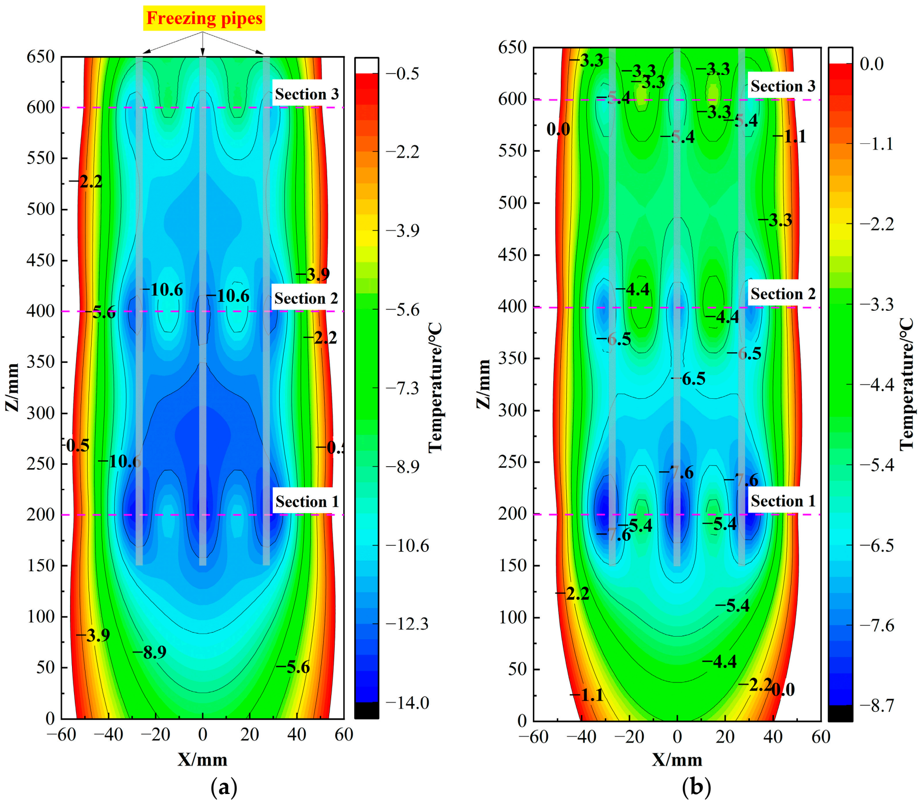

Figure 10. *Cont.*

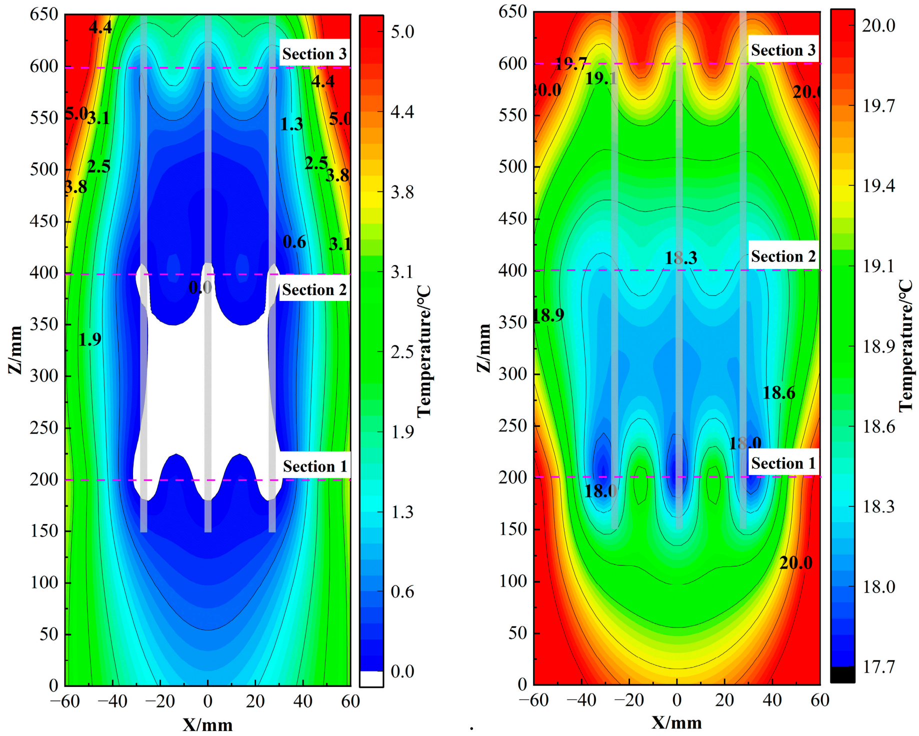

(**c**) (**d**)

Figure 10. Vertical temperature field after thawing for different times: (**a**) 0 min; (**b**) 5 min; (**c**) 15 min; (**d**) 85 min.

At the beginning of natural thawing, the frozen wall shows a different morphology at three sections, their thicknesses are 109.9, 104.4, and 101.2 mm, respectively, and the lowest temperature region is located between Section 1 and Section 2. After thawing for 5 min, the lowest-temperature region remained unchanged, and the thickness of the frozen wall in three sections shows Section 1 > Section 2 > Section 3, with width sizes of 101.0, 100.6, and 98.1 mm, respectively. Furthermore, there is not a great difference between the two values of Section 1 and Section 2, which is consistent with the horizontal temperature field. Furthermore, the thawing rates were 1.78, 0.76, and 0.62 mm/s, indicating that Section 1 at the beginning of thawing had the best thawing effect under the influence of the temperature gradient. After thawing for 15 min, the frozen soil only existed between Section 1 and Section 2, and the isotherm at Section 2 appears to "expand" to both sides due to the gradual decrease in the temperature gradient on the outside of the freezing pipes with the thawing time and the dissipation of the cold inside the frozen soil, leading to a decrease in the thawing rate. After thawing for 85 min, the lowest-temperature region remains unchanged due to Section 2 being in the middle position of the frozen wall, where the permafrost layer has a weaker ability to exchange heat with the outside world. Compared with other sections, its frozen area is the largest, and it takes more time to completely restore the unfrozen soil.

By analyzing the vertical temperature field and frozen wall morphology at three sections of the freezing pipe, it is found that the soil temperature along the length direction of the freezing pipe shows non-uniformity. The temperature of the pipe walls in three sections after thawing for 5, 15, 48, and 85 min was selected and fitted to further study the temperature distribution law of the freezing pipe wall. The fitting curves of the temperature distribution under the different times of thawing are shown in Figure 11.

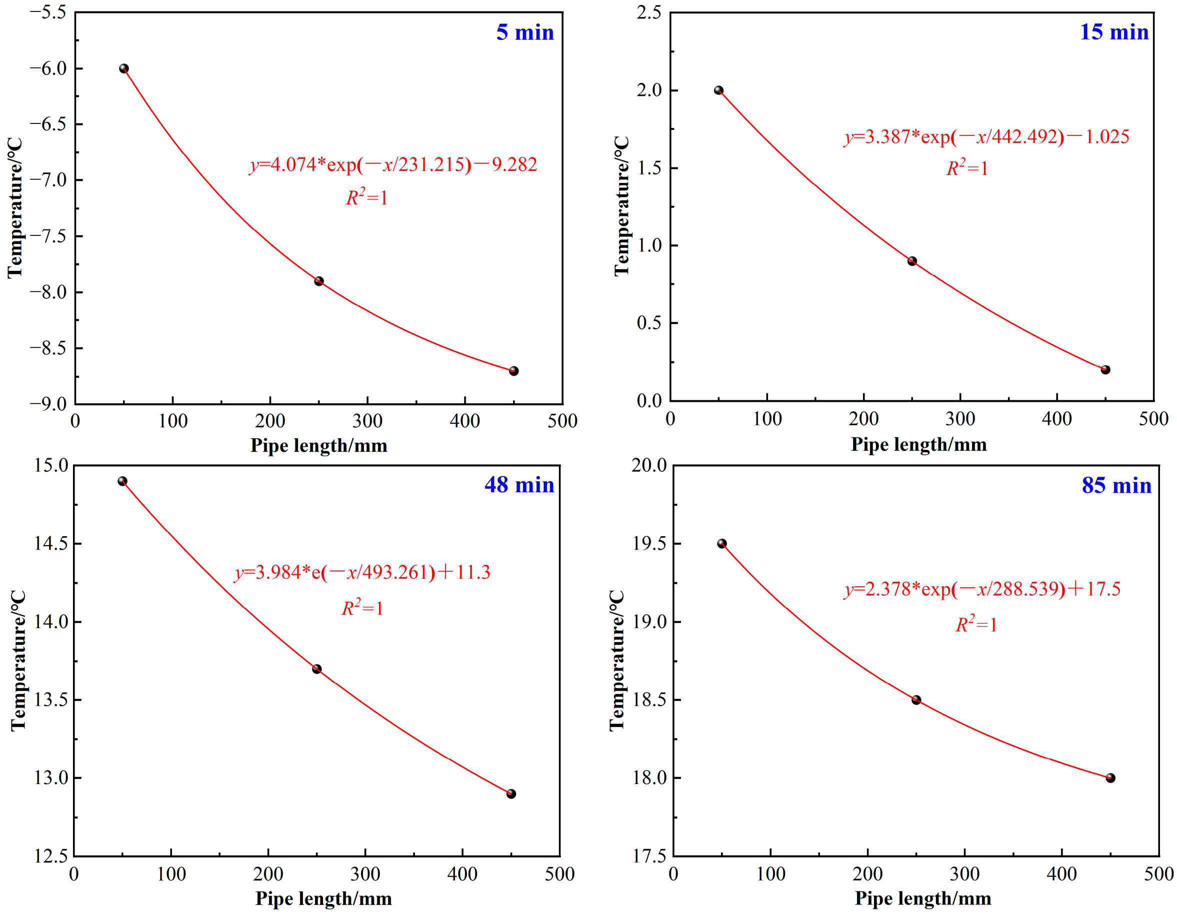

Figure 11. Fitting curves of pipe wall temperature along pipe length after thawing at different times.

As shown in Figure 11, in the natural thawing process, the evolution of the freezing pipe wall temperature in the direction of the vertical pipe diameter is not a simple linear change, and there are differences in the rate of temperature change at the three sections, such as the wall temperature at Section 2 has the smallest growth rate with thawing time.

When a single exponential decay function is used, the distribution function at each time along the pipe length direction is

$$\begin{cases} T_5(l) = 4.074\exp(-l/231.215) - 9.282 \ \ , t = 5\text{min} \\ T_{15}(l) = 3.387\exp(-l/442.492) - 1.025 \, , t = 15\text{min} \\ T_{48}(l) = 3.984\exp(-l/493.261) + 11.3 \ , t = 48\text{min} \\ T_{85}(l) = 2.378\exp(-l/288.539) + 17.5 \ , t = 85\text{min} \end{cases} \tag{10}$$

where T indicates the pipe wall temperature, °C, and l indicates the pipe length, mm. This function can provide model parameters for the subsequent development of related numerical simulation studies.

4. Discussion

This experiment only investigated the evolution law of the thawing temperature field in homogeneous strata and the non-uniform distributions law along the length of the freezing pipe, and the freezing method used was vertical freezing with casing-type freezing pipes. However, the distribution of strata in actual engineering is complex and the freezing method is uncertain, and the laws obtained in this paper have limited applications. We will consider the randomness of the formation distribution based on the random medium theory in the subsequent study, construct a prediction model for the inhomogeneous thawing temperature field of complex formations, verify it using numerical methods, and carry out further research on the thawing settlement effects generated by it.

5. Conclusions

Based on the hygrothermal coupling similarity criterion, an artificial ground freezing test platform was built to study the formation and melting laws of frozen walls under vertical freezing conditions, and the following main results and conclusions are drawn.

(1) During the positive freezing period, the temperature changes at each measurement point went through three stages: A steep drop, a slow drop, and basic stability, while during the natural thawing period, there were four stages, namely, a rapid rise, a short lag, a second rapid rise, and a linear slow rise.
(2) After 61 min of positive freezing, the thickness of the frozen wall on different sections showed Section 1 > Section 2 > Section 3. After 85 min of natural thawing, the size of the area where the ground temperature was not restored showed that Section 2 > Section 1 > Section 3, and the thawing effect of the stratum in the middle of the freezing pipe was the worst.
(3) The distribution of the natural thawing temperature field is non-uniform along the length of the pipe, and the pipe wall temperature along this direction is distributed as an exponential function, which can provide a theoretical basis for subsequent numerical simulation study of the three-dimensional non-uniform thawing temperature field.

Author Contributions: Conceptualization, H.C.; Methodology, C.L.; Formal analysis, L.Y.; Data curation, C.P., M.L. and R.H.; Writing – original draft, L.Y.; Writing – review & editing, M.L.; Funding acquisition, H.C. All authors have read and agreed to the published version of the manuscript.

Funding: This research was supported by the National Natural Science Foundation of China (Grant No. 51778004); Academic Funding for Top-notch Talents in University Disciplines (Majors) of Anhui Province, China (Grant No. gxbjZD10); Research on Graduate Science Project in Anhui Province, China (No. YJS20210383); the Graduate Innovation Fund Project of Anhui University of Science and Technology (2020CX2024); and the Graduate Innovation Fund Project of Anhui University of Science and Technology (2022CX2047). In addition, Haibing Cai is responsible for the derivation of theoretical equations and technical guidance, Longfei Yang is responsible for the model test and thesis writing; and Changqiang Pang, Mengkai Li, Chanrui Lu, and Rongbao Hong are responsible for the test and data processing.

Data Availability Statement: The datasets generated and analyzed during the current study are available from the corresponding author upon reasonable request.

Conflicts of Interest: The authors declare that there are no conflicts of interest regarding the publication of this paper.

References

1. Chen, R.J.; Cheng, G.D.; Li, S.X.; Guo, X.M.; Zhu, L.N. Development and prospect of research on application of artificial ground freezing. *Chin. J. Geotech. Eng.* **2000**, *1*, 43–47.
2. Pimentel, E.; Papakonstantinou, S.; Anagnostou, G. Numerical interpretation of temperature distributions from three ground freezing applications in urban tunnelling. *Tunn. Undergr. Space Technol.* **2012**, *28*, 57–69. [CrossRef]
3. Zaid, M.; Sadique, M.R.; Alam, M.M. Blast Resistant Analysis of Rock Tunnel Using Abaqus: Effect of Weathering. *Geotech. Geol. Eng.* **2022**, *40*, 809–832. [CrossRef]
4. Zheng, L.F.; Gao, Y.T.; Zhou, Y.; Liu, T.; Tian, S.G. A practical method for predicting ground surface deformation induced by the artificial ground freezing method. *Comput. Geotech.* **2021**, *130*, 103925. [CrossRef]
5. Cheng, H.; Yao, Z.S.; Zhang, J.S.; Rong, C.X. A model test study on the effect of freeze heaving and thaw subsidence for tunnel construction with artificial horizontal ground freezing. *China Civ. Eng. J.* **2007**, *10*, 80–85.
6. Yang, P.; Chen, M.H.; Zhang, W.M.; Zhao, H.G.; Yu, C.H. Observation of the Forming and Thawing of Frozen Walls. *J. Glaciol. Geocryol.* **1998**, *20*, 128–132.
7. Hu, X.D.; Fang, T.; Guo, X.D.; Ren, H. Temperature field research on thawing process of Freeze-Sealing Pipe Roof Method in Gongbei Tunnel by in-situ prototype test. *J. China Coal Soc.* **2017**, *42*, 1700–1705.
8. Hu, X.D.; Wu, Y.H.; Li, X.Y. A Field Study on the Freezing Characteristics of Freeze-Sealing Pipe Roof Used in Ultra-Shallow Buried Tunnel. *Appl. Sci.* **2019**, *9*, 1532. [CrossRef]

9. Ma, J.; Yang, P.; Liu, Z.G.; Li, Z.Y.; Chen, L. Study on Thawing Law of the Connecting Passage in Changzhou Sandy Formation. *Chin. J. Undergr. Space Eng.* **2019**, *15*, 168–173+180.
10. Levin, L.; Gelovatyi, I.; Zaitsev, A.; Pugin, A.; Semin, M. Thermal monitoring of frozen wall thawing after artificial ground freezing: Case study of Petrikov Potash Mine. *Tunn. Undergr. Space Technol.* **2021**, *107*, 103685.
11. Li, F.Z.; Xia, M.P. Study on analytical solution of temperature field of artificial frozen soil by exponent-integral function. *J. Southeast Univ. (Nat. Sci. Ed.)* **2004**, *34*, 469–473.
12. Jiang, B.S.; Wang, J.G.; Zhou, G.Q. Analytical Calculation of Temperature Field Around a Single Freezing Pipe. *J. China Univ. Min. Technol.* **2009**, *38*, 463–466.
13. Zhang, C.; Yang, W.H.; Qi, J.G.; Zhang, T. Analytic computation on the forcible thawing temperature field formed by a single heat transfer pipe with unsteady outer surface temperature. *J. Coal Sci. Eng. (China)* **2012**, *18*, 18–24.
14. Cai, H.B.; Peng, L.M.; Zheng, T.L. A duration prediction model of surface thawing settlement in construction period of tunnel with horizontal freezing method. *Rock Soil Mech.* **2014**, *35*, 504–510.
15. Cai, H.B.; Peng, L.M.; Zheng, T.L. A method for predicting ground surface settlement in the artificial thawing period of tunnel horizontally frozen wall. *Rock Soil Mech.* **2015**, *36*, 3516–3522+3530.
16. Harlan, R.L. Analysis of coupled heat- fluid transport in partially frozen soil. *Water Resour. Res.* **1973**, *19*, 1314–1323. [CrossRef]
17. Chen, X.B.; Wang, Y.Q. Frost heave prediction for clayey soils. *Cold Reg. Sci. Technol.* **1988**, *15*, 233–238.
18. Shen, M.; Branko, L. Modelling of coupled heat, moisture and stress field in freezing soil. *Cold Reg. Sci. Technol.* **1990**, *14*, 237–246.
19. Yuan, Y.H.; Yang, P. Numerical Analysis of Soil Thermal Field in Freezing Reinforcement of Shield Arriving. *Chin. J. Undergr. Space Eng.* **2010**, *6*, 1053–1059.
20. Chen, C.; Yang, P.; Zhang, T. Numerical Analysis of Artificial Thawing Temperature Field in High-confined Aquifer Reinforcement. *J. Zhengzhou Univ. (Eng. Sci.)* **2012**, *33*, 81–85.
21. Fu, Y.; Hu, J.; Liu, J.; Hu, S.B.; Yuan, Y.H.; Zeng, H. Finite Element Analysis of Natural Thawing Heat Transfer of Artificial Frozen Soil in Shield-Driven Tunnelling. *Adv. Civ. Eng.* **2020**, *2020*, 2769064. [CrossRef]
22. Zhou, J.; Tang, Y.Q. Centrifuge experimental study of thaw settlement characteristics of mucky clay after artificial ground freezing. *Eng. Geol.* **2015**, *190*, 98–108.
23. Shi, R.J.; Yue, F.T.; Zhang, Y.; Lu, L. Model test on freezing reinforcement for shield junction Part 1: Distribution characteristics of temperature field in soil stratum during freezing process. *Rock Soil Mech.* **2017**, *38*, 368–375.
24. Hu, X.D.; Fang, T.; Chen, J.; Ren, H.; Guo, W. A large-scale physical model test on frozen status in freeze-sealing pipe roof method for tunnel construction. *Tunn. Undergr. Space Technol.* **2018**, *72*, 55–63.
25. Duan, Y.; Rong, C.X.; Cheng, H.; Cai, H.B.; Long, W. Freezing Temperature Field of FSPR under Different Pipe Configurations: A Case Study in Gongbei Tunnel, China. *Adv. Civ. Eng.* **2021**, *2021*, 9958165.